

Characterising large-scale structure with the REFLEX II cluster survey

Gayoung Chon¹

¹Max-Planck-Institut für extraterrestrische Physik
Garching 85748, Germany
email: gchon@mpe.mpg.de

Abstract. We study the large-scale structure with superclusters from the REFLEX X-ray cluster survey together with cosmological N-body simulations. It is important to construct superclusters with criteria such that they are homogeneous in their properties. We lay out our theoretical concept considering future evolution of superclusters in their definition, and show that the X-ray luminosity and halo mass functions of clusters in superclusters are found to be top-heavy, different from those of clusters in the field. We also show a promising aspect of using superclusters to study the local cluster bias and mass scaling relation with simulations.

Keywords. cosmology:large-scale structure of universe, X-rays: galaxies: clusters, methods: n-body simulations

1. Introduction

Superclusters are the largest overdense structures found in the galaxy and galaxy cluster surveys, defined in general as groups of two or more galaxy clusters above a certain density enhancement (Bahcall (1988)). Unlike clusters they have not reached a quasi-equilibrium configuration, hence the definition of superclusters must be made clear such that their properties can be studied quantitatively. One solution to this problem is to include the future evolution of superclusters into the definition of the object, selecting only those structures that will collapse in the future. This allows us to obtain a more homogeneous class of superclusters. We have been exploring this approach observationally using an appropriate selection criterion to construct an X-ray supercluster catalogue (Chon et al. (2013), Chon et al. (2014)). It is based on the REFLEX X-ray cluster survey, which provides the largest and homogeneous X-ray cluster sample to date in the southern sky (Böhringer et al. (2013), Chon & Böhringer (2012)). Since the REFLEX survey has a well-defined selection function, we can apply equivalent criteria to dark matter halos in cosmological N-body simulations to construct superclusters, which allows us to study superclusters more quantitatively.

2. Defining superclusters

To identify a region that will collapse in the future, we approximate the overdense regions by homogeneous density spheres, which has been successfully used in the literature for many applications. We can then model the evolution of the overdense region with respect to the expansion of the background cosmology with reference to Birkhoff's theorem. This allows us to describe the evolution of both the overdense and background regions by the respective values of the local and global Hubble constant, H , matter density, Ω_m , and Ω_Λ corresponding to a cosmological constant. We evolve both regions from

a starting redshift of 500, which results in an accuracy well below 1% in the final calculation. We solve the Friedmann equations for a spherical collapse model iteratively where the local matter density is enhanced at the starting redshift in the overdense region. We then obtain a criterion for R , which is the ratio between the minimally required local overdensity to the mean density of the universe today. This density ratio, for example, is 7.858 for the flat Λ CDM cosmology with $\Omega_m=0.3$ and $h=0.7$. Since we use a friends-of-friends (fof) algorithm to build superclusters from clusters, the linking length must reflect this required density ratio. Given that the linking length is inversely proportional to a third power of the local density of clusters, we find that the overdensity parameter, f , used in the fof algorithm has to be about 25 for a cluster bias of 2-3. In Chon et al. (2013) we adopted a slightly more generous value of ten for the nominal catalogue together with that built with $f=50$ for comparison so as to collect a slightly larger regions than just the core of the collapsing superclusters. We recover a number of known superclusters including Shapley, Hydra-Centaurus, and Aquarius B as well as a number of new X-ray superclusters. Based on our physically driven choice of the overdensity parameter, one of the consequences is that, for example, the Shapley supercluster is fragmented into three smaller mass concentrations. A further study of the radial profile of Shapley mass concentration implies that in fact approximately the central $11 \text{ h}^{-1} \text{ Mpc}$ of Shapley is under-going a collapse currently, while regions outside $13 \text{ h}^{-1} \text{ Mpc}$ will not collapse in the future despite the fact that the outskirts of Shapley are rich with clusters (Chon et al., submitted).

3. Superclusters as dark matter tracers

The fact that the REFLEX II supercluster sample has been constructed by means of a statistically well-defined sample of closely mass-selected clusters motivates us to search for a more precise physical characterisation of the superclusters in simulations. We achieve this by applying criteria equivalent to those used in our X-ray selection, and regard halos as clusters by imposing a mass limit to halos in the Millennium simulation (Springel (2005)). Our nominal lower mass limit is $10^{14} \text{ h}^{-1} \text{ M}_\odot$ corresponding to a typical mass limit of a cluster survey, and we construct superclusters with the same overdensity parameter that was used for the REFLEX II superclusters.

One of the interesting aspects in the study of superclusters is how superclusters trace the underlying dark matter. Since we have almost no direct access to determined their masses, an indirect mass estimate would still be helpful. Since we have mass estimates of the member clusters through mass-observable scaling relations, the total supercluster mass can be estimated if we can calibrate the cluster mass fraction in superclusters. Similarly we would be able to determine the dark matter overdensity traced by a supercluster if the mass fraction relation or the overdensity bias could be calibrated. Hence we consider two quantities, the mass fraction represented by the total clusters mass in a supercluster, and the bias of clusters in superclusters. A better knowledge of the former would allow us to make a prediction of the underlying total mass of a superclusters through a mass scaling relation like that of clusters.

The left panel of Fig. 1 shows the total cluster mass as a function of the total mass of superclusters with the best fit to a power-law shown in a solid line, which is enclosed by two dashed lines representing its two sigma scatter. The total mass of a supercluster is defined to be the sum of all halos in the volume with a correction factor that takes the particles which do not contribute to the halo mass, M_{200} , assuming that they are distributed throughout the volume in an unbiased way. The fact that the total cluster mass is closely correlated with the total halo mass of a supercluster gives a first encouraging

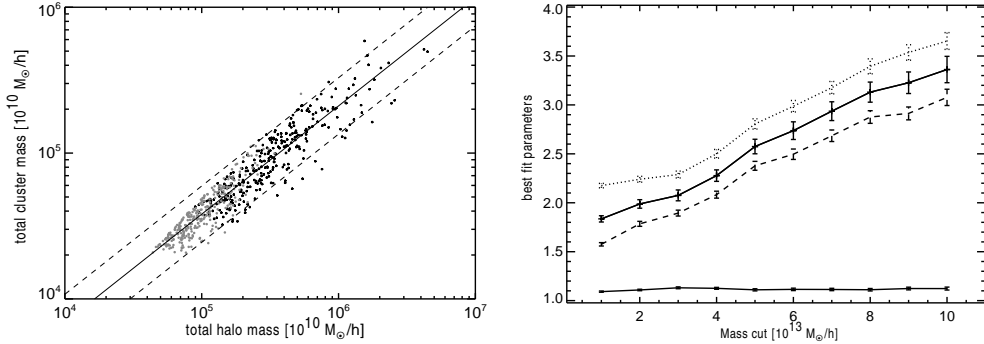


Figure 1. (Left) Total mass of a supercluster probed by the total mass of member clusters. The halos of the lower halo mass limit of $10^{14}h^{-1}M_{\odot}$ are considered here. (Right) Fitted slope and amplitude for the mass bias as a function of the mass limit in the cluster catalogue. In comparison we show the fitted amplitude of the pair (dotted) and richer (dashed) superclusters separately where the slope is fixed to that for the entire sample.

evidence that there is a potential to use the cluster observables to trace the dark matter distribution in the regions of superclusters.

The power spectrum of clusters of galaxies measures the density fluctuation amplitude of the distribution of clusters as a function of a scale, where the amplitude ratio of this power spectrum in comparison with the power spectrum of the dark matter is interpreted as a bias that clusters have. Analogous to the power spectrum of clusters, we take the number overdensity of clusters in superclusters as a measure of bias against the dark matter overdensity, for which we take again the halo mass overdensity as a tracer. This approach makes use of the observable, the number overdensity of clusters, so it can be calibrated against a quantity from simulations, the dark matter mass overdensity. In this case we consider a continuous range of lower halo mass limits from $10^{13}h^{-1}M_{\odot}$ to $10^{14}h^{-1}M_{\odot}$ to form ten cluster catalogues from the simulation and construct ten supercluster samples. We fit a power-law to the cluster number density as a function of the mass density of halos in superclusters. The best fit parameters are shown in the right panel of Fig. 1 where dotted and dashed lines represent those superclusters with two member clusters and richer superclusters. The uncertainties are calculated by one thousand bootstrappings of the sample. The fitted slope of this relation turns out to be nearly constant, ~ 1.1 , for all mass ranges of consideration, hence we interpret the fitted amplitude as a bias. We see that the bias increases with an increasing lower mass limit in a cluster catalogue, which is also expected. We note that for the $10^{14}h^{-1}M_{\odot}$ mass limit, the local bias is 3.36, and for the $10^{13}h^{-1}M_{\odot}$ it decreases to 1.83. This result is in line with the biases obtained from the power spectrum analysis, the former being 2.1 and the latter 3.3 (Balaguera-Antolinez et al. (2011)). The fair agreement between the cluster biases calculated locally and globally is encouraging because the cluster number overdensity clearly extends into non-linear regime whereas the calculated bias of the power spectrum is mainly based on linear theory. This motivates the next section where we will quantitatively test how much this non-linear environment differs from the field.

4. Supercluster environment

Cluster mass functions can be predicted on the basis of cosmic structure formation models such as the hierarchical clustering model for CDM universe (Press & Schechter (1974)). Due to the close relation of X-ray luminosity and gravitational mass of clusters the mass

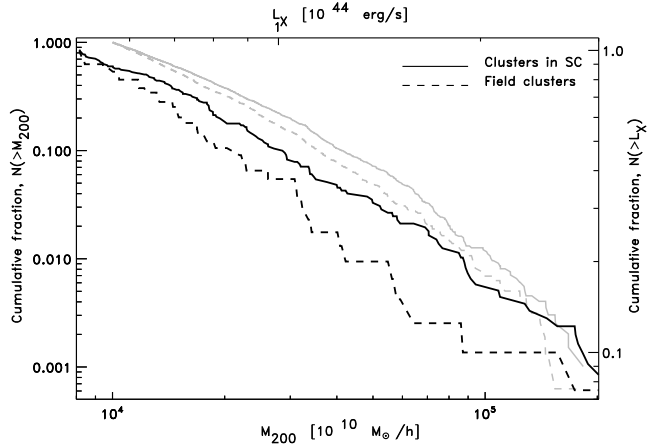


Figure 2. Measured cumulative X-ray luminosity function from REFLEX shown in thick black lines in comparison to the cumulative mass function of the superclusters in simulations in grey lines. In both cases clusters in superclusters are denoted by a solid line, while field clusters by dashed lines.

function is reflected by the X-ray luminosity function (XLF) of clusters. Thus we use the observed XLF as a substitute for the mass function. The clusters in superclusters are used separately to form their own XLF in comparison to those in the field, and to better illustrate the difference we consider a normalised cumulative luminosity function as shown in Fig. 2. The black lines represent the volume-limited sample of the REFLEX II clusters.

We see a clear effect that we have a more top-heavy luminosity function for the clusters in superclusters compared to those in the field. Since the cumulative distribution is unbinned, we quantify the difference with a Kolmogorov-Smirnov (KS) test yielding the probability, P , that both luminosity distributions come from the same parent distribution with a value of 0.03. With the Millennium simulation, we form the same cumulative distribution directly with masses shown in grey lines in Fig. 2. In this case the probability from the KS test is practically zero. Hence both in our REFLEX data and simulation that there are over-abundance of more luminous clusters in the superclusters than in the field.

References

Bahcall, N. 1988, *ARA&A*, 26, 631B
 Balaguera-Antolinez, A. 2011, *MNRAS*, 413, 386B
 Böhringer, H., Chon, G., Collins, C., Guzzo, L., Nowak, N., Bobrovsky, S. 2013, *A&A* 555, 30
 Böhringer, H., Chon, G., Collins, C. A. (2014) 2014, *A&A* in press
 Böhringer, H., Chon, G., Bristow, M., Collins, C. A. 2014, *A&A* submitted
 Chon, G. & Böhringer, H. 2013, *A&A*, 538, 35
 Chon, G., Böhringer, H., Nowak, N. 2013, *MNRAS*, 429, 3272
 Chon, G., Böhringer, H., Collins, C., Krause, M. 2014, *A&A*, 567, 144
 Chon, G., Böhringer, H., Zaroubi, S. 2014, *A&A* submitted
 Press, W. H., & Schechter, P. 1974, *ApJ*, 187, 425
 Springel, V. 2005, *MNRAS*, 364, 1105